

# Aligned bioactive mesoporous silica coatings for implants

J. M. GOMEZ-VEGA\*, H. SUGIMURA, O. TAKAI

*Department of Materials Processing Engineering, Graduate School of Engineering, Nagoya University, Furo-cho, Chikusa-ku, Nagoya 464-8603, Japan*

A. HOZUMI

*National Industrial Research Institute of Nagoya, 1-1 Hirate-cho, Kita-ku, Nagoya 462-8510, Japan*

*Email: jose@plasma.numse.nagoya-u.ac.jp*

Ongoing research is reported aimed at preparing mesoporous silica coatings on various substrates for medical applications by a biomimetic approach (self-assembling of organic/inorganic sol-gel systems into ordered structures). Tetraethylorthosilicate (TEOS) was selected as the silica precursor, and amphiphilic triblock copolymers poly(ethylene oxide)-poly(propylene oxide)-poly(ethylene oxide), and the cationic surfactant cetyltrimethyl ammonium chloride (CTAC), as structure-directing agents. The mesochannels diameter could be adjusted by changing the directing agent, and a preferred alignment of the mesostructure was observed independently of the used substrate (glass, silicon, Ti or Ti6Al4V). Three different treatments (thermocalcination, photocalcination, and solvent extraction) have been also studied to remove the organic templates, of which photocalcination showed to be the most versatile. When soaked in a simulated body fluid, mesoporous silica coatings induced apatite formation after seven days.

© 2001 Kluwer Academic Publishers

## Introduction

Inorganic oxides (e.g. silica) can be arranged in ordered mesoporous structures when precursors (usually alkoxides) polymerize in the presence of self-assembling directing agents, typically surfactants or amphiphilic polymers [1–5]. Compared to conventional low molecular weight surfactants, self-assembly of amphiphilic block copolymers can result in mesostructured materials with larger pore sizes (up to 30 nm) [4]. Once the organic part has fulfilled its role as template for the formation of the ordered inorganic frame (commonly, it can exhibit cubic or hexagonal packing, depending on the system and conditions used) [6–8], it is eliminated (usually by a thermal treatment) leaving the imprint of their original presence. Lamellae structures can be also formed, but they collapse after thermocalcination.

Recently, mesoporous thin films have been synthesized so far by the virtue of their technological potentiality as membranes, sensors, heterogeneous catalysis or insulating layers of low dielectric constant for microelectronics [9]. In this work, the application of mesoporous silica films on several substrates by spin coating of templated sol-gel solutions has been investigated as an approach to coatings with nanoscaled structures that may be used in medical applications.

## Experimental methods

Plates (10 × 10 × 1 mm) of micro-slide glass, Ti, Ti6Al4V, and silicon (Mitsubishi Material Silicon Co.) were used as substrates to be coated. The plates were ultrasonically cleaned in acetone and ethanol before the spin coating process. Silicon substrates were additionally etched in HF (5 vol %) for ~ 30 s to remove the silica layer. Amphiphilic triblock copolymers poly(ethylene oxide)-poly(propylene oxide)-poly(ethylene oxide) type (HO(CH<sub>2</sub>CH<sub>2</sub>O)<sub>n</sub>(CH<sub>2</sub>CH(CH<sub>3</sub>O))<sub>m</sub>(CH<sub>2</sub>CH<sub>2</sub>O)<sub>n</sub>H) Pluronic L-121 (EO<sub>4-5</sub>PO<sub>60</sub>EO<sub>4-5</sub>), and P-123 (EO<sub>20</sub>PO<sub>70</sub>EO<sub>20</sub>), were provided by BASF, and used as received. Sol-gel solutions with triblock copolymers were prepared with the following molar ratio: polymer 0.017:TEOS 1:HCl 6:H<sub>2</sub>O 167. A sol with the cationic surfactant cetyltrimethyl ammonium chloride (CH<sub>3</sub>(CH<sub>2</sub>)<sub>15</sub>N(CH<sub>3</sub>)<sub>3</sub>Cl) (CTAC) was also prepared with the composition: CTAC 1.1:TEOS 1:HCl 70:H<sub>2</sub>O 1000. The mesoporous silica films were applied over the substrates by spin coating of the sols described above. The thicknesses of the coatings could be varied between approximately 0.1 and 1 μm by changing the rotating speed. The specimens were allowed to dry overnight at room temperature. Three different methods were evaluated to remove the organic component of the coatings: (i) Thermocalcination: firing in air between 300

\* Author to whom correspondence should be addressed.

to 500 °C: (ii) photocalcination: ultraviolet irradiation in air with an excimer lamp ( $\lambda = 172$  nm) for different periods and pressures; (iii) solvent extraction: soaking in a refluxing solution of HCl (37 wt%) and methanol (1:7 wt) for 24 h (specimens with metallic substrates were not treated with this method).

The coating surfaces were examined by scanning electron microscopy with associated energy dispersive spectroscopy analysis (SEM-EDS) with an apparatus Jeol JSM-6330F. X-ray diffraction (XRD) analyses were accomplished with a Rigaku 2100 instrument using nickel-filtered  $\text{CuK}_\alpha$  radiation. A Biorad FTS 175C Fourier transformed infrared (FT-IR) transmission spectrometer was used to estimate the elimination of the organic template after the different treatments and conditions.

To evaluate the capacity of the coatings to precipitate apatite during *in vitro* tests, the specimens were introduced in polyethylene containers with 20 ml of simulated body fluid (SBF), and placed in a water bath with the temperature fixed at 37 °C. The SBF was prepared by dissolving reagent-grade NaCl, KCl,  $\text{CaCl}_2$ ,  $\text{MgCl}_2 \cdot 6\text{H}_2\text{O}$ ,  $\text{NaH}_2\text{CO}_3$ ,  $\text{K}_2\text{HPO}_4$  and  $(\text{CH}_2\text{OH})_3\text{CNH}_2$  in distilled water, and buffering it at  $\text{pH} = 7.25$  with HCl. After soaking, the coatings were rinsed with distilled water and dried in air at room temperature.

## Results and discussion

Mesoscopic ordering of the spin-casted silica-copolymer coatings was characterized by low angle XRD. The XRD patterns of as-deposited silica coatings on glasses using the triblock copolymer P-123 as directing agent are shown in Fig. 1. Five well-resolved peaks indexable as ( $h00$ ) reflections associated with hexagonal symmetry are observed. A combination of electrostatic and hydrogen bonding between silicon species in the sol and the organic template are presumed to be responsible for the assembly of silica into hexagonal arrays of mesochannels [10]. The absence of XRD (110) reflections indicates that the  $c$ -axis of the hexagonal unit cell is oriented parallel to the substrate surface, which means that the mesochannels of the coatings run parallel to the substrate [11]. The mesostructure of the self-assembled organic/inorganic frames depended directly on the molecular weight and sterical volume of the organic template used. Accordingly, silica films with well-ordered channels of the same diameter in the  $\sim 3$ – $13$  nm regime could be prepared through this templated assisted sol-gel process simply by changing the directing agent.

A preferred alignment of the mesostructure can explain the variation of the diffraction peak intensities that is observed when the samples are rotated azimuthally (within the plane  $x$ - $y$ ; Fig. 1) [11]. In the case of crystalline substrates such as silicon [11], graphite [12], or mica [13], the micelle rods of the directing agent can be accommodated in a preferred direction following an “epitaxial-like” growth of the mesoporous silica film. A mechanism that explains oriented mesoporous silica films on amorphous substrates like glass is not evident, although it must be remarked that the effect of the

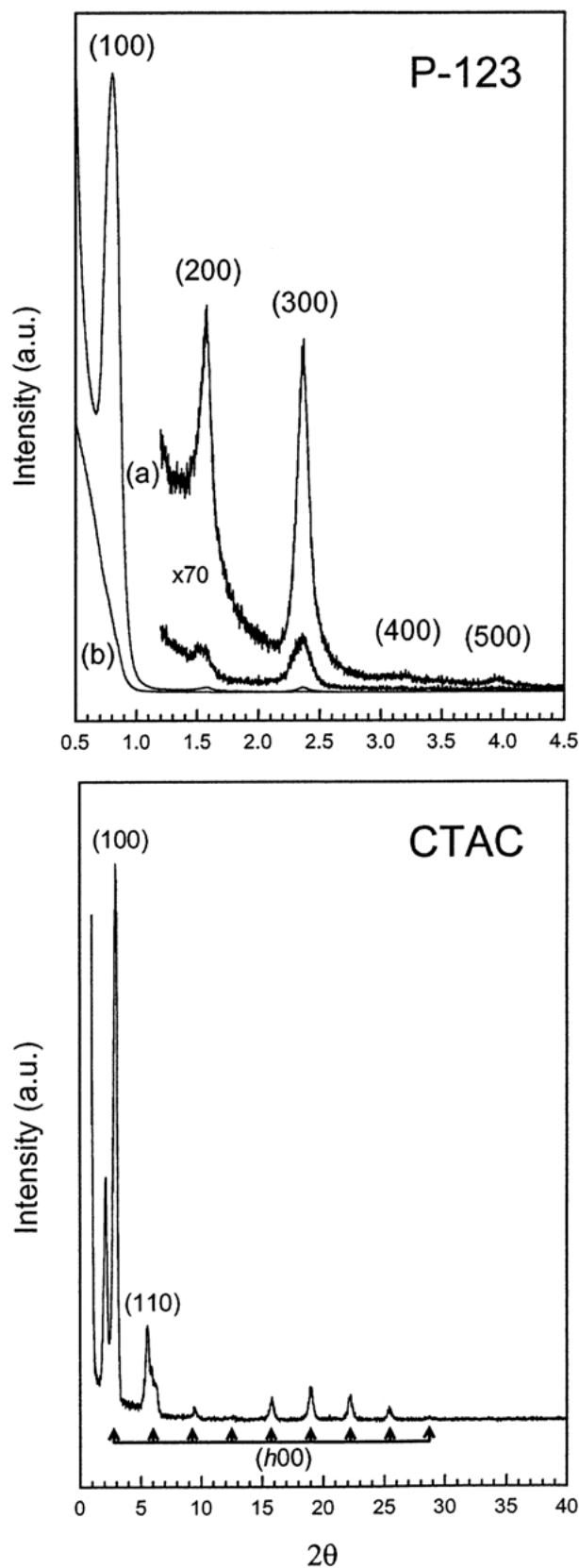


Figure 1 Low angle XRD patterns of as-deposited silica films on glass using the triblock copolymer P-123 as directing agent. The diffractograms correspond to (a) the sample orientation where peaks were most intense, and (b) after rotating the sample azimuthally 90°. Lower part shows the XRD spectrum of as-deposited mesoporous silica coating on silicon using CTAC as directing agent.

substrate on the mesoporous film is less important in the case of using fast coating techniques, like spin coating, than in the case of slower ones, such as dipping. The rheology of the sol-gel solutions prepared in this work is

fundamentally governed by the block copolymers because the gel formation, which may impede their motion, scarcely occurs in the conditions of restrained hydrolysis and condensation of the silicon alkoxide (TEOS) used in this work. Besides, polymeric materials undergo dramatic changes in orientational order in response to dynamic processes [14], and block copolymers are recognized for their tendency to form well-ordered periodic microstructures, often with exceptionally intricate geometries [15]. In consequence, the spinning process and/or the formation of regular, dissipative structures caused by convection during the evaporation of the solvent, may be the causes that induce a preferred orientation in the nucleation and growth of the mesochannels [16]. Mesoporous silica films prepared using CTAC as directing agent are not preferentially aligned (the diffraction peaks intensities did not change when rotating the samples). The existence of the (110) reflection is also expected in the case of a more randomly oriented mesoporous structure [13]. The reason may be that CTAC is a small cationic surfactant that is not severely affected by dynamic processes or by different responses of any of its constituents as in the case of block copolymers.

The contraction of the  $d_{100}$  spacing (increasing of  $2\theta$ ) and the decrease of the diffraction intensity, that happens when coatings were treated to remove the organic material (Fig. 2), implies that the structures underwent further condensation of residual hydroxyl groups that

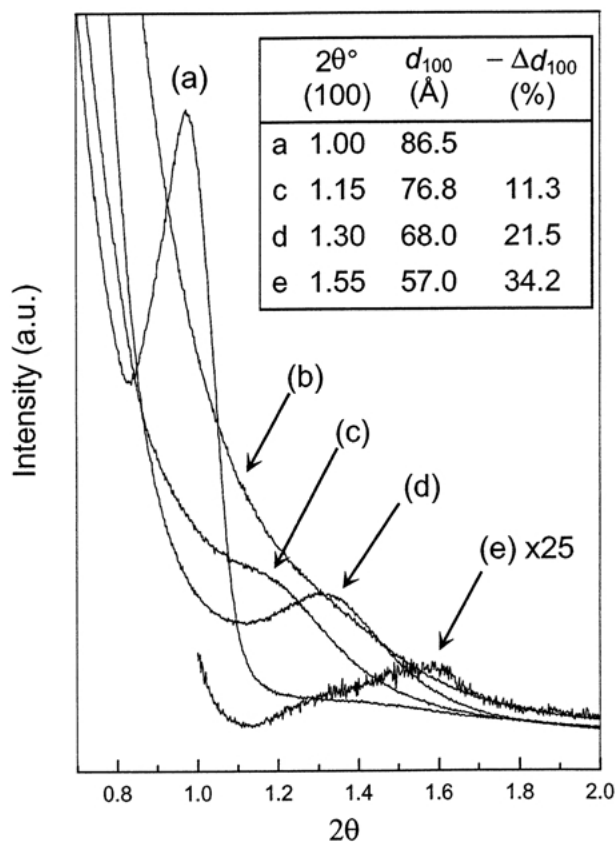


Figure 2 Low angle XRD spectra of as-deposited silica film on silicon using the triblock copolymer L-121 as directing agent: (a) as-prepared; (b) thermocalcined ( $500^\circ\text{C}/1^\circ\text{Cmin}^{-1}/1\text{ h}$ ) or photocalcined ( $1000\text{ Pa}/1\text{ h}$ ); (c) after solvent extraction (HCl and methanol at reflux for 24 h); (d) thermocalcined ( $300^\circ\text{C}/1^\circ\text{Cmin}^{-1}/1\text{ h}$ ) and (e) photocalcined ( $10\text{ Pa}/3\text{ h}$ ).

resulted in disordering of the mesostructure. Although chemical extraction was the least aggressive method –  $\Delta d_{100} = 11.3\%$ , it is the most laborious and cannot be used with metallic specimens because they are attacked by strong acids. In the case of thermocalcination, some oxidation occurs at the edges of the specimens. The capacity to eliminate the organic component and its effect on the mesostructure depended highly on the conditions of the thermo- and photo-calcination treatments (Fig. 3). Firings up to  $500^\circ\text{C}$  were necessary to remove completely the organic part of the coatings. In the case of photocalcination, the C–C bonds cleavage kinetics was increased when the atmosphere was richer in oxygen (higher pressure), and consequently the removal of the organic part of the coatings was more

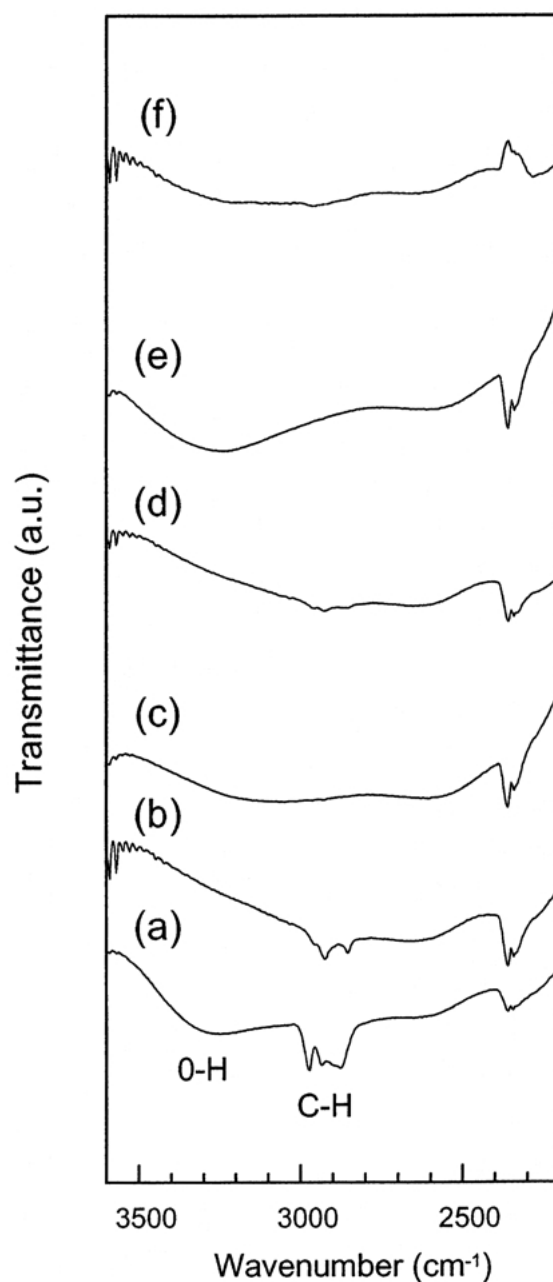


Figure 3 FT-IR spectra of silica films on glass using the triblock copolymer L-121 as directing agent: (a) as-prepared; (b) thermocalcined ( $300^\circ\text{C}/1^\circ\text{Cmin}^{-1}/3\text{ h}$ ); (c) thermocalcined ( $500^\circ\text{C}/1^\circ\text{Cmin}^{-1}/1\text{ h}$ ); (d) photocalcined ( $10\text{ Pa}/3\text{ h}$ ); (e) photocalcined ( $1000\text{ Pa}/1\text{ h}$ ) and (f) after solvent extraction (HCl and methanol at reflux for 24 h).

efficient and resulted in more silanol groups on the samples (Fig. 3). The presence of silanols is a good indication about the potential ability of the coatings to induce apatite formation when soaked in SBF. Nevertheless, an excessively rapid photooxidation induces an abrupt rearrangement of the film structure and the loss of the mesoscopic order (Fig. 2). Therefore, a compromise should be found between the conditions used to remove the organic part, particularly air pressure, presence of silanols, and ordered mesoporosity. Since photo-induced cleavage of any C–C bonds can eliminate any organic molecules (including bacteria), the specimens are perfectly sterilized after its application, which may be important in the case of implants. Moreover, the excimer lamp does not generate infrared rays so photocalcination occurs at room temperature and deleterious reactions with the metallic substrates are avoided [17].

The essential condition for a material to bond with living bone (bioactive behavior) is the formation of apatite on its surface in the body environment, as previous studies with glasses and glass–ceramics *in vivo* and *in vitro* have demonstrated [18–20]. Mesoporous silica coatings on Ti6Al4V photooxidized at 100 Pa for 2 h tested *in vitro* showed the presence of apatite crystals precipitating on the surface after 7 days of immersion in SBF (Fig. 4). Li *et al.* [21–24] have proved that even pure silica fabricated by a sol–gel route can precipitate apatite when tested in SBF. The rate of apatite formation was shown to depend on pH, concentration of ions in solution and sintering temperature of the gel–silica, and it was suggested that the silanol groups present on the surface might be responsible for the apatite formation. Furthermore, Karlsson *et al.* [25] indicated that, as opposed to dense silica and durable silicate glasses, the gel–silica may be flexible enough to provide the oxide–oxide spatial requirement to match the bone apatite lattice, thereby providing epitaxial sites for bone growth. According to previous studies, the texture (pore size and volume) exerts a great effect on the rate of apatite formation on gel–silica surfaces [26], and a great mesopore volume and a wide mesopore size distribution favor hydroxycarbonate apatite nucleation [27]. However, Cho *et al.* [28] speculate that the presence of certain type of structural unit of silanol groups is the main factor for inducing apatite formation. A mechanism that assumes pores as nucleation sites was proposed by Pereira *et al.* [26] who suggest that nucleation of apatite occurs likely inside the pores through the establishment of an electrical double layer with higher ionic concentration. The presence of silanols is also justified in this mechanism because rehydration and establishment of the electrical double layer depends on this parameter. The proposed mechanism would imply that, when ordered mesostructures are present, as in the samples prepared in this work, apatite should nucleate in the regular pattern established by the alignment of the mesochannels. Both the mesoporous structure and/or the surface rich in silanol groups can explain the observed formation of apatite on the mesoporous silica films prepared in this work, but we could not determine any relation between the rate of apatite formation and the pore size or silanol presence. Nevertheless, ongoing

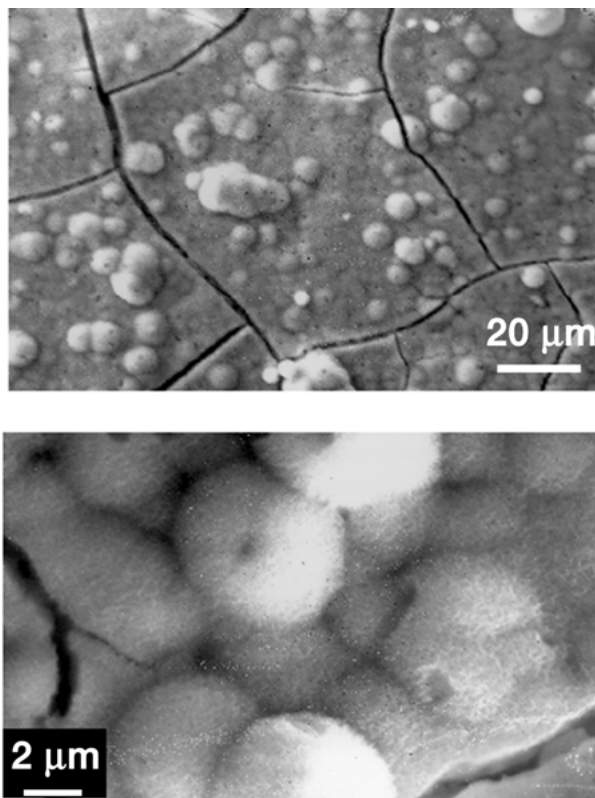


Figure 4 SEM photograph of the formed apatite on silica films applied on Ti6Al4V soaked in SBF for seven days. Hemispherical formations with a leaf-like texture can be observed.

work is focused on the early stages of formation of apatite *in vitro*, and more precise measurements may shed light on the mechanism responsible for apatite formation, particularly in the role of porosity and silanol contents. Since the crystallite size of hydroxyapatite in bone ( $25 \times 2.5\text{--}5 \text{ nm}^2$ ) is in the mesoscopic regime accessible through the methodology described here, certain orienting effect of these substrates on the formed hydroxyapatite could be expected to occur, which might be critical in the strength of the interface developed with the bone.

## Conclusions

The fabrication of metallic substrates coated with bioactive silica, with a preferred alignment of the mesochannels and the appropriate range of pore size, may be a valid route to enhance the implant's performance. These coatings may induce fast osseointegration and result in long lasting implants due to the formation of hydroxyapatite and collagen structures with a preferred alignment at the implant/bone interface.

## Acknowledgments

Work supported by JSPS-RFTF no. 99R13101 "Biomimetic Materials Processing," and Spanish Ministry of Education and Culture (MEC).

## References

1. J. S. BECK, J. C. VARTULI, W. J. ROTH, M. E. LEONOWICZ, C. T. KRESGE, K. D. SCHMITT, C. T.-W. CHU, D. H. OLSON,

- E. W. SHEPPARD, S. B. MCCULLEN, J. B. HIGGINS and J. L. SCHLENKER, *J. Am. Chem. Soc.* **114** (1992) 10834.
2. A. MONNIER, F. SCHUTH, Q. HUO, D. KUMAR, D. MARGOLESE, R. S. MAXWELL, G. D. STUCKY, M. KRISHNAMURTY, P. PETROFF, A. FIROUZI, M. JANICKE and B. F. CHMELKA, *Science* **261** (1993) 1299.
  3. I. AKSAY, M. TRAU, S. MANNE, I. HONMA, N. YAO, L. ZHOU, P. FENTER, P. M. EISENBERGER and S. M. GRÜNER, *ibid.* **273** (1996) 892.
  4. D. ZHAO, J. FENG, Q. HUO, N. MELOSH, G. H. FREDRICKSON, B. F. CHMELKA and G. D. STUCKY, *ibid.* **279** (1998) 548.
  5. J. WEN and G. L. WILKES, *Chem. Mater.* **8** (1996) 1667.
  6. U. CIESLA and F. SCHUTH, *Micropor. Mesopor. Mater.* **27** (1999) 131.
  7. Q. HUO, D. I. MARGOLESE and G. D. STUCKY, *Chem. Mater.* **8** (1996) 1147.
  8. Y. S. LEE, D. SURJADI and J. F. RATHMAN, *Langmuir* **16** (2000) 195.
  9. S. PEVZNER, O. REGEV and R. YERUSHALMI-ROZEN, *Curr. Opin. Colloid Interf. Sci.* **4** (2000) 420.
  10. P. YANG, D. ZHAO, D. I. MARGOLESE, B. F. CHMELKA and G. D. STUCKY, *Chem. Mater.* **11** (1999) 2813.
  11. H. MIYATA and K. KURODA, *J. Am. Chem. Soc.* **121** (1999) 7618.
  12. H. YANG, N. COOMBS, I. SOKOLOV and G. A. OZIN, *J. Mater. Chem.* **7** (1997) 1285.
  13. H. YANG, A. KUPERMAN, N. COOMBS, S. MAMICHE- AFARA and G. A. OZIN, *Nature* **379** (1996) 703.
  14. R. H. COLBY, *Curr. Opin. Colloid Interf. Sci.* **1** (1996) 454.
  15. M. W. MATSEN, *ibid.* **3** (1998) 40.
  16. O. KARTHAUS, L. GRASJO, N. MARUYAMA and M. SHIMOMURA, *Thin Solid Films* **829** (1998) 327.
  17. J. M. GOMEZ-VEGA, E. SAIZ and A. P. TOMSIA, *J. Biomed. Mater. Res.* **46** (1999) 549.
  18. T. KOKUBO, S. ITO, Z. T. HUANG, T. HAYASHI, S. SAKKA, T. KITSUGI and T. YAMAMURO, *J. Biomed. Mater. Res.* **24** (1990) 331.
  19. L. D. WARREN, A. E. CLARK and L. L. HENCH, *J. Biomed. Mater. Res. Appl. Biomater.* **23** (1989) 201.
  20. P. LI, I. KANGASNIEMI, K. DE GROOT and T. KOKUBO, *J. Am. Cer. Soc.* **77** (1994) 1307.
  21. P. LI, I. KANGASNIEMI, K. DE GROOT, T. KOKUBO and A. U. YLI-URPO, *J. Non-Cryst. Solids* **168** (1994) 281.
  22. P. LI, I. KANGASNIEMI, K. DE GROOT and T. KOKUBO, *Biomaterials* **14** (1993) 963.
  23. P. LI, C. OHTSUKI, T. KOKUBO, K. NAKANISHI, N. SOGA and K. DE GROOT, *J. Biomed. Mater. Res.* **28** (1994) 7.
  24. C. P. A. T. KLEIN, P. LI, J. M. A. DE BLIECK-HOGERVORST and K. DE GROOT, *Biomaterials* **16** (1995) 715.
  25. K. H. KARLSSON, K. FROBERG and T. J. RINGBOM, *J. Non-Cryst. Solids* **112** (1989) 69.
  26. M. M. PEREIRA, A. E. CLARK and L. L. HENCH, *J. Am. Cer. Soc.* **78** (1995) 2463.
  27. T. PELTOLA, M. JOKINEN, H. RAHIALA, E. LEVANEN, J. B. ROSENHOLM, I. KANGASNIEMI and A. U. YLI-URPO, *J. Biomed. Mater. Res.* **44** (1998) 12.
  28. S. B. CHO, F. MIYAJI, T. KOKUBO, K. NAKANISHI, N. SOGA and T. NAKAMURA, *J. Mater. Sci. Mater. Med.* **9** (1998) 279.

*Received 14 May  
and accepted 23 May 2001*